Science and Technology Indonesia
e-ISSN:2580-4391 *p*-ISSN:2580-4405
Vol. 11, No. 3, July 2026

Research Paper

Check for updates

Numerical Solution of the Gardner Equation Using the Method of Lines and an Improved Fifth-Order Runge-Kutta Scheme

Dismahayuna Pratyamifta Naisya Putri[1], and Ummu Habibah[1*]

[1]*Department of Mathematics, Faculty of Mathematics and Natural Sciences, Universitas Brawijaya, Malang, East Java 65145, Indonesia*
***Corresponding author**: ummu_habibah@ub.ac.id

Abstract
The Gardner equation is a nonlinear partial differential equation that arises in the modeling of nonlinear dispersive wave phenomena. Analytical solutions of this equation are limited to specific cases, which motivates the development of reliable numerical approaches. This study presents a numerical scheme based on the Method of Lines combined with an Improved Runge-Kutta method of order five to solve the Gardner equation. Spatial discretization is performed using second-order central finite difference schemes, which transform the governing equation into a system of ordinary differential equations. The resulting system is integrated in time using the fifth-order Improved Runge-Kutta method to achieve high accuracy and computational efficiency. Simulations targeting solitary pulse and kink-like wave solutions reveal that the MOL-IRK5 scheme consistently outperforms the classical MOL-RK4 method. The numerical results show strong agreement with the exact solutions at all observed time levels. Wave profiles are preserved during propagation, and no spurious oscillations are observed. Global error measures, including the maximum error, mean absolute error, and root mean square error, remain small throughout the simulation interval, indicating stable numerical performance. The results demonstrate that the proposed MOL-IRK5 scheme provides accurate and efficient approximations for different types of Gardner equation solutions. The numerical approach presented in this study offers a reliable framework for solving nonlinear dispersive equations and can be extended to more complex mathematical models in applied science and engineering.

Keywords
Gardner Equation, Method of Lines, Improved Runge-Kutta Method, Solitary Pulse, Kink-Like Wave, Numerical Simulation

Received: 29 January 2026, Accepted: 22 April 2026
https://doi.org/10.26554/sti.2026.11.3.903-914

1. INTRODUCTION

The Gardner equation is a nonlinear partial differential equation that combines the quadratic nonlinearity of the Korteweg-de Vries equation and the cubic nonlinearity of the modified Korteweg-de Vries equation. This equation plays an important role in modeling nonlinear wave phenomena arising in various physical applications, including shallow water waves, plasma physics, and layered fluid systems (Khater, 2024). Analytical solutions of the Gardner equation are only available for specific cases and initial conditions, while most practical problems require numerical approximations due to the nonlinear and dispersive nature of the equation (Wazwaz, 2009).

Various numerical approaches have been developed to approximate solutions of the Gardner equation (Gardner, 2024; Dahiya et al., 2023; Hepson et al., 2018; Zhang et al., 2025). Spectral and pseudospectral methods are known for their high accuracy but often involve complex implementations and relatively high computational costs (Bacca et al., 2023). Collocation methods based on spline functions have also been applied and shown to produce accurate numerical solutions with available exact solutions for comparison (Hepson et al., 2020). Finite difference-based approaches combined with the Method of Lines reduce the partial differential equation into a system of ordinary differential equations and provide a simpler and more practical numerical framework (Boyce and DiPrima, 2012). Previous studies commonly employ classical time integration schemes such as the fourth-order Runge-Kutta method in the Method of Lines approach, which has been shown to be stable and effective for solving the Gardner equation (Tiong et al., 2017).

Recent developments in high-order time integration methods for nonlinear partial differential equations, such as exponential time differencing and advanced Runge-Kutta schemes, have demonstrated improved accuracy and efficiency in solving dispersive wave equations (Cox and Matthews, 2002; Kassam and Trefethen, 2005; Shu, 2009). These approaches provide a strong foundation for developing efficient numerical frameworks for nonlinear wave propagation problems.

Limited studies have explored the use of higher-order efficient time integration schemes within the Method of Lines framework for the Gardner equation (Ji and Xing, 2023; Keppens et al., 2023). Applications that simultaneously consider different types of exact solutions, such as solitary pulse and kink-like wave solutions, remain scarce in the literature. Recent developments indicate that higher-order schemes such as the modified Exponential Time Differencing Runge-Kutta method can achieve high accuracy, although at the cost of increased computational complexity (Degon and Chowdhury, 2022). An alternative approach is the Improved Runge-Kutta method of order five, which reduces the number of function evaluations while preserving fifth-order global accuracy, making it a promising candidate for efficient numerical simulations (Habibah et al., 2025).

To the best of our knowledge, this study presents one of the first systematic implementations of the Method of Lines combined with an Improved Fifth-Order Runge-Kutta scheme for solving the Gardner equation. The primary motivation for this study is to overcome the accuracy limitations of the standard RK4 while maintaining better computational efficiency than IRK5 schemes. Unlike existing numerical studies that rely on classical fourth-order Runge-Kutta or spectral-based approaches, the proposed MOL-IRK5 framework offers higher-order time integration with improved computational efficiency while retaining numerical stability. Furthermore, this work simultaneously investigates solitary pulse and kink-like wave solutions and evaluates numerical performance using comprehensive global error measures. The results demonstrate that the proposed approach provides accurate and reliable approximations for different wave structures of the Gardner equation.

2. NUMERICAL METHOD

This study employs a numerical approach to solve the Gardner equation by combining spatial discretization using the Method of Lines with a high order time integration scheme. No physical materials or laboratory equipment are involved, as the investigation is entirely computational and analytical in nature. The numerical procedures are implemented to evaluate the accuracy and efficiency of the proposed scheme through comparison with known exact solutions.

2.1 Mathematical Model

The Gardner equation is a nonlinear evolution equation that combines the quadratic nonlinearity of the Korteweg-de Vries equation and the cubic nonlinearity of the modified Korteweg-de Vries equation. It is widely used to describe nonlinear dispersive wave propagation in shallow water, plasma physics, and layered fluid systems. The Gardner's equation is written in Equation (1):

$$u_t + \mu_1 u u_x + \mu_2 u^2 u_x + \mu_3 u_{xxx} = 0, \tag{1}$$

where $u(x,t)$ denotes the wave profile, x and t denote the spatial and temporal variables, respectively, and parameters μ_1, μ_2, μ_3 describe nonlinear and dispersive effects (Wazwaz, 2009).

In this study, Equation (1) is solved subject to an initial condition

$$u(x,0) = u_0(x). \tag{2}$$

Equation (2) is taken from the corresponding exact solution of the Gardner equation for either a solitary pulse or a kink-like wave. Homogeneous Neumann boundary conditions are imposed at both ends of the computational domain as stated in Equation (3),

$$\frac{du}{dx}(a,t) = 0, \quad \frac{du}{dx}(b,t) = 0, \tag{3}$$

to ensure numerical stability and physical consistency.

The spatial domain is discretized using a uniform grid, and spatial derivatives are approximated by second-order central finite difference schemes. Through the Method of Lines (MOL), the governing partial differential equation is transformed into a system of ordinary differential equations,

$$\frac{dU}{dx} = F(U), \tag{4}$$

where U denotes the vector of nodal solution values. The resulting system in Equation (4) is integrated in time using an Improved Runge-Kutta method of order five (IRK5), which provides high accuracy with reduced computational cost compared to conventional Runge-Kutta schemes.

This formulation enables efficient and accurate numerical simulation of the Gardner equation and forms the basis for evaluating solitary pulse and kink-like wave solutions in the present study.

2.2 Spatial Discretization and Semi-Discrete Formulation

To apply the Method of Lines, the spatial domain $[a,b]$ is discretized into N grid points, with x_i expressed in Equation (5).

$$x_i = a + i\Delta x. \tag{5}$$

The first spatial derivative is approximated using the central difference formula

$$u_x(x_i,t) \approx \frac{u_{i+1} - u_{i-1}}{2\Delta x} \tag{6}$$

The third derivative is approximated by

$$u_{xxx}(x_i,t) \approx \frac{u_{i-2} - 2u_{i-1} + 2u_{i+1} - u_{i+2}}{2\Delta x^3} \tag{7}$$

Substituting these approximations in Equations (6) and (7) into the Gardner Equation (1) yields a semi-discrete system of ordinary differential equations

$$\frac{du_i}{dt} = F(u_{i-2}, u_{i-1}, u_i, u_{i+1}, u_{i+2}), \tag{8}$$

where $u_i(t)$ denotes the numerical approximation of $u(x_i, t)$. This formulation reduces the original partial differential equation into a system of ordinary differential equations that depend only on time.

2.3 Time Integration Using the Improved Runge–Kutta Method

The resulting system of ordinary differential equations is solved using an Improved Rung-Kutta method of order five (IRK5). This method provides fifth-order accuracy while requiring fewer function evaluations compared to conventional high-order Runge-Kutta schemes.

Boundary conditions are implemented using ghost points derived from the Neumann conditions to preserve numerical stability near the domain boundaries. In the discrete equation at the lower boundary, a fictitious or ghost point u_0 appears. To eliminate this point, a homogeneous Neumann boundary condition is applied, which states that the spatial derivative at the lower boundary is zero: $u_x(a, t) = 0$. Using a central difference approximation, this derivative is expressed in Equation (9).

$$u_x(a, t) \approx \frac{u_2(t) - u_0(t)}{2h} = 0. \tag{9}$$

From Equation (9), it follows that $u_0(t) = u_2(t)$, allowing the ghost point to be replaced by values within the physical domain. Similarly, at the upper boundary, a ghost point $u_{(M+1)}$ is introduced. The homogeneous Neumann condition $u_x(b, t) = 0$ is applied to ensure the spatial derivative at the boundary is zero. Using the central difference approach:

$$u_x(b, t) \approx \frac{u_{(M+1)}(t) - u_{(M-1)}(t)}{2h} = 0. \tag{10}$$

Based on Equation (10), we obtain $u_{(M+1)}(t) = u_{(M-1)}(t)$. By substituting this relation back into the governing equations, the fictitious point $u_{(M+1)}$ is effectively eliminated while maintaining second-order accuracy at the boundary.

The iterative process for advancing the solution from y_i to $y_{(i+1)}$ is defined by the following weighted average of five slope estimates given in Equation (11) (Habibah et al., 2025):

$$y_{(i+1)} = y_i + \frac{1}{6}k_1 + \frac{1}{3}k_2 + \frac{1}{3}k_3 + \frac{1}{10}k_4 + \frac{1}{15}k_5, \tag{11}$$

where each intermediate slope k_n is calculated sequentially given in Equations (12)-(16):

$$k_1 = hf(t_i, y_i), \tag{12}$$

$$k_2 = hf(t_i + \frac{1}{2}h, y_i + \frac{1}{2}k_1), \tag{13}$$

$$k_3 = hf(t_i + \frac{1}{2}h, y_i + \frac{1}{2}k_2), \tag{14}$$

$$k_4 = hf(t_i + h, y_i + k_3), \tag{15}$$

$$k_5 = hf(t_i + h, y_i + \frac{1}{2}k_1 + \frac{1}{2}k_4). \tag{16}$$

2.4 Numerical Stability

The numerical stability of the proposed MOL-IRK5 scheme depends on both spatial discretization and time integration. In this study, spatial derivatives are approximated using second-order central finite difference schemes, while temporal integration is performed using the Improved Runge-Kutta method of order five.

For nonlinear dispersive equations such as the Gardner equation, stability is influenced by the relationship between the spatial grid size Δx and the time step Δt. In practical computations, the time step is selected sufficiently small relative to the spatial step size to maintain stable numerical integration.

In the present simulations, the time step satisfies.

$$\Delta t \leq C\Delta x \tag{17}$$

where C is a constant depending on the nonlinear wave propagation characteristics. The conditions in Equation (17) ensures that the numerical solution remains stable and accurately resolves the wave dynamics.

3. RESULTS AND DISCUSSION

Numerical simulations are performed to evaluate the performance of the proposed Method of Lines combined with the Improved Runge-Kutta method of order five (MOL-IRK5) in solving the Gardner equation. Two representative types of solution are considered, namely the solitary pulse and the kink-like wave. These solutions represent different wave characteristics and provide useful benchmarks for assessing the accuracy and stability of the numerical scheme (Kai et al., 2024). The numerical solutions are compared with the corresponding exact solutions at several time levels. The comparison allows evaluation of the ability of the proposed method to preserve wave shape, amplitude, and propagation characteristics over time. The accuracy of the numerical solutions is evaluated by comparing them with the corresponding exact solutions at selected time levels. Three global error measures are employed, namely the maximum error, the mean absolute error, and the root mean square error. These error metrics provide a quantitative assessment of the reliability and performance of the proposed numerical scheme (Trisilowati et al., 2021). The Improved Runge-Kutta method of order five offers a favorable balance between accuracy and computational efficiency, requiring fewer function evaluations than classical fifth-order schemes while maintaining global fifth-order accuracy.

3.1 Numerical Results for the Solitary Pulse Case

The solitary pulse case is examined using the parameter values $\mu_1 = 4$, $\mu_2 = -3$, and $\mu_3 = 1$, which correspond to a localized traveling wave solution of the Gardner equation. The spatial domain is defined as $x \in [-20, 30]$ with a uniform spatial step size $\Delta x = 0.5$, while the temporal discretization is set to $\Delta t = 0.1$. The temporal step size is chosen to maintain numerical stability and accuracy of the time integration scheme. In the simulations, the time step satisfies the relation

$$\Delta t = 0.1\Delta x \tag{18}$$

Equation (18) ensures stable numerical integration and adequate temporal resolution of the wave propagation.

The exact solutions considered in this study are the solitary pulse and the kink-like wave. The initial condition is obtained directly from the exact solitary pulse solution at the initial time. The simulation parameters are summarized in Table 1. Visual inspection of the solitary pulse at $t = 1$, $t = 5$, and $t = 10$ reveals that both the MOL-RK4 and MOL-IRK5 schemes overlap significantly with the exact solution, effectively capturing the peak and the symmetric decay of the pulse. While both methods show high fidelity, the magnified view at the wave crest suggests that the MOL-IRK5 method tracks the exact solution with a slightly higher degree of precision as the simulation time increases.

The comparison between numerical and exact solutions at different time levels shows that the numerical solution accurately reproduces the exact wave profile throughout the simulation Yang (2024) as shown in Figure 1.

The solitary wave propagates along the spatial domain without distortion of its shape or amplitude, indicating that the numerical scheme preserves the essential characteristics of the solitary pulse. The agreement between numerical and exact solutions remains strong at later times, showing that the proposed method maintains accuracy throughout the simulation interval (Wu and Zhao, 2024). Quantitative analysis provided in Table 1 further supports this, showing that at t=1, the absolute errors for both methods are remarkably small, typically in the range of 10^{-5} to 10^{-7}. Specifically, at certain spatial points such as x = -17.5 and x = -16, the MOL-IRK5 scheme demonstrates a lower absolute error compared to the classical MOL-RK4, confirming its enhanced accuracy in resolving the Gardner equation's dynamics.

The small magnitude of the global error measures confirms the high accuracy and stability of the MOL-IRK5 numerical scheme. The maximum error means absolute error, and root means square error exhibit a gradual increase as time progresses, which is expected due to the accumulation of discretization errors. The numerical accuracy is evaluated using several error norms including the E_∞, E_R, and E_K norms defined in Equations (19)-(21).

$$E_\infty = \max\left|u_i^{num} - u_i^{exact}\right| \tag{19}$$

$$E_R = \frac{1}{N}\sum_{i=1}^{N}\left|u_i^{num} - u_i^{exact}\right| \tag{20}$$

$$E_K = \sqrt{\frac{1}{N}\sum_{i=1}^{N}\left(u_i^{num} - u_i^{exact}\right)^2} \tag{21}$$

These results demonstrate that the MOL-IRK5 scheme provides accurate approximations for the solitary pulse solution of the Gardner equation. A summary of the numerical results for some observation times is given in Table 2 and Table 3.

3.2 Numerical Results for the Kink-Like Wave Case

The kink-like wave case is investigated using the parameter values $\mu_1 = 1$, $\mu_2 = -5$, and $\mu_3 = 1$, which generate a kink-like traveling wave solution of the Gardner equation. The spatial domain is defined as $x \in [-80, 80]$ with a uniform spatial step size $\Delta x = 0.5$, and the time step is set to $\Delta t = 0.1$. The exact solutions considered in this study are the solitary pulse and the kink-like wave. The initial condition is obtained from the exact kink-like wave solution at the initial time. The simulation setting for the kink-like wave case is listed in Table 4.

The numerical solution accurately reproduces the kink-like wave profile and maintains strong agreement with the exact solution throughout the simulation interval san shwon in Figure 2. Visual analysis of the wave propagation at t=1, t=10, and t=20 indicates that both MOL-RK4 and MOL-IRK5 effectively capture the monotonic transition of the kink wave. The magnified insets in Figure 2 demonstrate that the IRK5 scheme follows the exact solution curve with minimal deviation, even as the wave progresses over longer time intervals.

The transition region of the wave is captured smoothly, and the numerical solution remains consistent with the exact solution throughout the simulation interval. The wave propagates along the spatial domain without generating spurious oscillations near the transition region, demonstrating that the numerical scheme effectively handles solutions with sharp gradients (Neto et al., 2022). Quantitative data from Table 2 at t=1 confirms the superior precision of the proposed methods, with absolute errors remarkably low, ranging between 10^{-8} and 10^{-10}. For instance, at x = -79 and x = 76, the MOL-IRK5 scheme consistently yields absolute errors in the magnitude of

Table 1. Comparison between Exact and Numerical Solutions, and Absolute Error at Time t = 1 for The Solitary Pulse Case

$x(i)$	Exact	MOL-RK4	MOL-IRK5	Absolute Error MOL-RK4	Absolute Error MOL-IRK5
-20.0	8.250×10^{-5}	8.561×10^{-5}	8.561×10^{-5}	3.11×10^{-6}	3.11×10^{-6}
-19.5	9.745×10^{-5}	1.1510×10^{-4}	1.1511×10^{-4}	1.76×10^{-5}	1.77×10^{-5}
-19.0	1.1512×10^{-4}	1.2894×10^{-4}	1.2885×10^{-4}	1.38×10^{-5}	1.37×10^{-5}
-18.5	1.3598×10^{-4}	1.4123×10^{-4}	1.4133×10^{-4}	5.26×10^{-6}	5.35×10^{-6}
-18.0	1.6061×10^{-4}	1.6662×10^{-4}	1.6665×10^{-4}	6.01×10^{-6}	6.04×10^{-6}
-17.5	1.8971×10^{-4}	1.9012×10^{-4}	1.8993×10^{-4}	4.11×10^{-6}	2.18×10^{-7}
-17.0	2.2407×10^{-4}	2.2723×10^{-4}	2.2747×10^{-4}	3.16×10^{-6}	3.40×10^{-6}
-16.5	2.6464×10^{-4}	2.6335×10^{-4}	2.6325×10^{-4}	1.29×10^{-6}	1.39×10^{-6}
-16.0	3.1255×10^{-4}	3.1480×10^{-4}	3.1465×10^{-4}	2.25×10^{-6}	2.10×10^{-6}
-15.5	3.6910×10^{-4}	3.6722×10^{-4}	3.6755×10^{-4}	1.89×10^{-6}	1.55×10^{-6}
25.5	3.9741×10^{-4}	4.0245×10^{-4}	4.0286×10^{-4}	5.03×10^{-6}	5.44×10^{-6}
26.0	3.3653×10^{-4}	3.3477×10^{-4}	3.3502×10^{-4}	1.76×10^{-6}	1.50×10^{-6}
26.5	2.8495×10^{-4}	2.7550×10^{-4}	2.7512×10^{-4}	9.45×10^{-6}	9.84×10^{-6}
27.0	2.4127×10^{-4}	2.2627×10^{-4}	2.2625×10^{-4}	1.50×10^{-5}	1.50×10^{-5}
27.5	2.0428×10^{-4}	1.8829×10^{-4}	1.8856×10^{-4}	1.60×10^{-5}	1.57×10^{-5}
28.0	1.7295×10^{-4}	1.6159×10^{-4}	1.6148×10^{-4}	1.14×10^{-5}	1.15×10^{-5}
28.5	1.4642×10^{-4}	1.4503×10^{-4}	1.4494×10^{-4}	1.39×10^{-6}	1.48×10^{-6}
29.0	1.2396×10^{-4}	1.3660×10^{-4}	1.3669×10^{-4}	1.26×10^{-5}	1.27×10^{-5}
29.5	1.0494×10^{-4}	1.3378×10^{-4}	1.3379×10^{-4}	2.88×10^{-5}	2.88×10^{-5}
30.0	8.884×10^{-5}	8.561×10^{-5}	8.561×10^{-5}	3.23×10^{-6}	3.23×10^{-6}

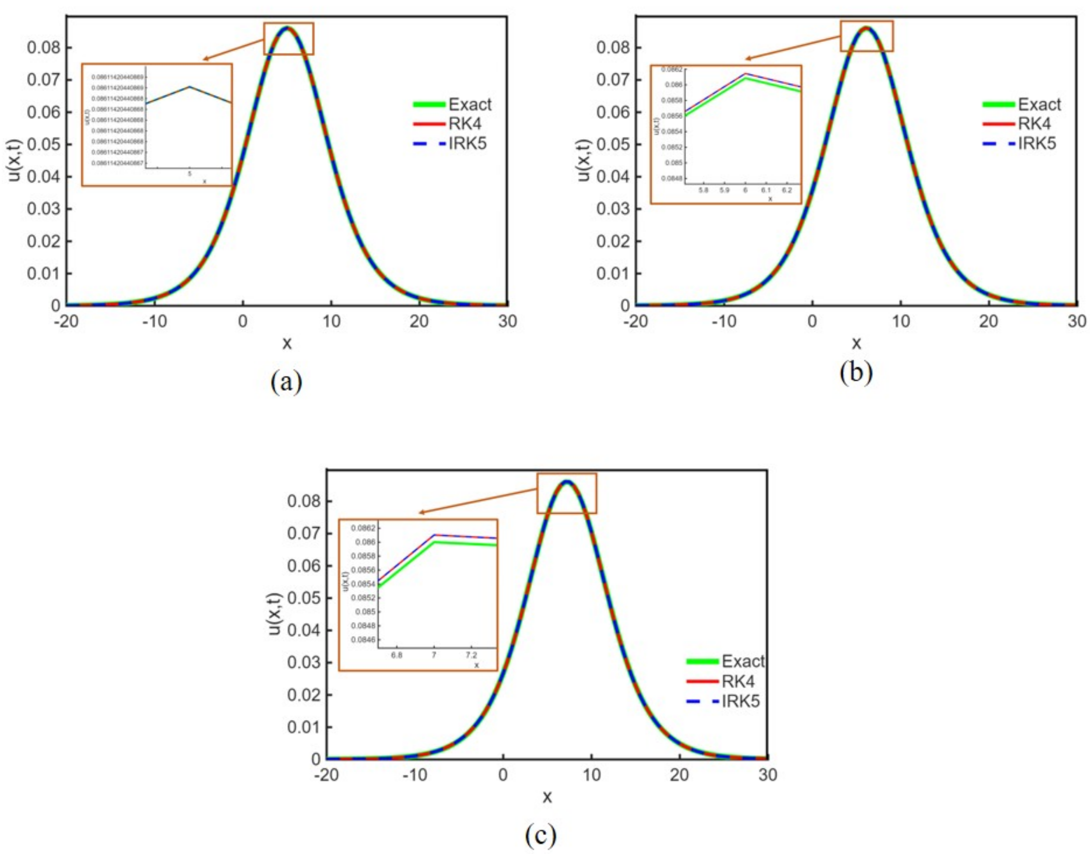

Figure 1. Exact and Numerical Solutions of the Gardner Equation Solitary Pulse for δx = 0.5 at (a) t = 1, (b) t = 5, and (c) t = 10

Table 2. Comparison between Exact and Numerical Solutions, and Absolute Error at Time $t = 5$ for The Solitary Pulse Case

$x(i)$	Exact	MOL-RK4	MOL-IRK5	Absolute Error MOL-RK4	Absolute Error MOL-IRK5
-20.0	7.114×10^{-5}	8.561×10^{-5}	8.561×10^{-5}	1.45×10^{-5}	1.45×10^{-5}
-19.5	8.404×10^{-5}	1.1995×10^{-4}	1.2003×10^{-4}	3.59×10^{-5}	3.60×10^{-5}
-19.0	9.927×10^{-5}	1.2816×10^{-4}	1.2834×10^{-4}	2.89×10^{-5}	2.91×10^{-5}
-18.5	1.1727×10^{-4}	1.3689×10^{-4}	1.3675×10^{-4}	1.96×10^{-5}	1.95×10^{-5}
-18.0	1.3852×10^{-4}	1.5514×10^{-4}	1.5491×10^{-4}	1.66×10^{-5}	1.64×10^{-5}
-17.5	1.6361×10^{-4}	1.7432×10^{-4}	1.7433×10^{-4}	1.07×10^{-5}	1.07×10^{-5}
-17.0	1.9325×10^{-4}	2.0299×10^{-4}	2.0334×10^{-4}	9.74×10^{-6}	1.01×10^{-5}
-16.5	2.2825×10^{-4}	2.3296×10^{-4}	2.3316×10^{-4}	4.71×10^{-6}	4.91×10^{-6}
-16.0	2.6958×10^{-4}	2.7462×10^{-4}	2.7422×10^{-4}	5.05×10^{-6}	4.65×10^{-6}
-15.5	3.1838×10^{-4}	3.2063×10^{-4}	3.2015×10^{-4}	2.26×10^{-6}	1.77×10^{-6}
25.5	4.6070×10^{-4}	4.4298×10^{-4}	4.4201×10^{-4}	1.77×10^{-5}	1.87×10^{-5}
26.0	3.9014×10^{-4}	3.7878×10^{-4}	3.7836×10^{-4}	1.14×10^{-5}	1.18×10^{-5}
26.5	3.3036×10^{-4}	3.1947×10^{-4}	3.2023×10^{-4}	1.09×10^{-5}	1.01×10^{-5}
27.0	2.7973×10^{-4}	2.7512×10^{-4}	2.7538×10^{-4}	4.62×10^{-6}	4.36×10^{-6}
27.5	2.3685×10^{-4}	2.3283×10^{-4}	2.3279×10^{-4}	4.02×10^{-6}	4.06×10^{-6}
28.0	2.0053×10^{-4}	2.0411×10^{-4}	2.0309×10^{-4}	3.57×10^{-6}	2.56×10^{-6}
28.5	1.6978×10^{-4}	1.7695×10^{-4}	1.7744×10^{-4}	7.17×10^{-6}	7.66×10^{-6}
29.0	1.4374×10^{-4}	1.6334×10^{-4}	1.6398×10^{-4}	1.96×10^{-5}	2.02×10^{-5}
29.5	1.2169×10^{-4}	1.5066×10^{-4}	1.5015×10^{-4}	2.90×10^{-5}	2.85×10^{-5}
30.0	1.0302×10^{-4}	8.561×10^{-5}	8.561×10^{-5}	1.74×10^{-5}	1.74×10^{-5}

Table 3. Comparison between Exact and Numerical Solutions, and Absolute Error at Time $t = 10$ for The Solitary Pulse Case

$x(i)$	Exact	MOL-RK4	MOL-IRK5	Absolute Error MOL-RK4	Absolute Error MOL-IRK5
-20.0	5.912×10^{-5}	8.561×10^{-5}	8.561×10^{-5}	2.65×10^{-5}	2.65×10^{-5}
-19.5	6.984×10^{-5}	1.1408×10^{-4}	1.1291×10^{-4}	4.42×10^{-5}	4.31×10^{-5}
-19.0	8.250×10^{-5}	1.1305×10^{-4}	1.1257×10^{-4}	3.06×10^{-5}	3.01×10^{-5}
-18.5	9.745×10^{-5}	1.1918×10^{-4}	1.2081×10^{-4}	2.17×10^{-5}	2.34×10^{-5}
-18.0	1.1512×10^{-4}	1.3052×10^{-4}	1.3025×10^{-4}	1.54×10^{-5}	1.51×10^{-5}
-17.5	1.3598×10^{-4}	1.4947×10^{-4}	1.4895×10^{-4}	1.35×10^{-5}	1.30×10^{-5}
-17.0	1.6061×10^{-4}	1.7271×10^{-4}	1.7200×10^{-4}	1.21×10^{-5}	1.14×10^{-5}
-16.5	1.8971×10^{-4}	1.9951×10^{-4}	2.0074×10^{-4}	9.80×10^{-6}	1.10×10^{-5}
-16.0	2.2407×10^{-4}	2.3132×10^{-4}	2.3146×10^{-4}	7.25×10^{-6}	7.39×10^{-6}
-15.5	2.6464×10^{-4}	2.6825×10^{-4}	2.6763×10^{-4}	3.61×10^{-6}	2.99×10^{-6}
25.5	5.5411×10^{-4}	5.2159×10^{-4}	5.2126×10^{-4}	3.25×10^{-5}	3.29×10^{-5}
26.0	4.6929×10^{-4}	4.4226×10^{-4}	4.4340×10^{-4}	2.70×10^{-5}	2.59×10^{-5}
26.5	3.9741×10^{-4}	3.7012×10^{-4}	3.7136×10^{-4}	2.73×10^{-5}	2.61×10^{-5}
27.0	3.3653×10^{-4}	3.1704×10^{-4}	3.1559×10^{-4}	1.95×10^{-5}	2.09×10^{-5}
27.5	2.8495×10^{-4}	2.6885×10^{-4}	2.6816×10^{-4}	1.61×10^{-5}	1.68×10^{-5}
28.0	2.4127×10^{-4}	2.4044×10^{-4}	2.4016×10^{-4}	8.34×10^{-7}	1.11×10^{-6}
28.5	2.0428×10^{-4}	2.1654×10^{-4}	2.1796×10^{-4}	1.23×10^{-5}	1.37×10^{-5}
29.0	1.7295×10^{-4}	2.0768×10^{-4}	2.0806×10^{-4}	3.47×10^{-5}	3.51×10^{-5}
29.5	1.4642×10^{-4}	1.9758×10^{-4}	1.9642×10^{-4}	5.12×10^{-5}	5.00×10^{-5}
30.0	1.2396×10^{-4}	8.561×10^{-5}	8.561×10^{-5}	3.83×10^{-5}	3.83×10^{-5}

10^{-9} and 10^{-10}, illustrating its high-order accuracy in maintaining the steep gradient of the kink structure.

The agreement between numerical and exact solutions persists at later times, indicating that the proposed numerical method maintains stability and accuracy for the kink-like wave case (Rugg et al., 2024). These observations confirm that the MOL-IRK5 scheme is robust when applied to Gardner equation solutions with non-symmetric and monotonic wave structures. A summary of the numerical results for some observation times is given in Table 5 and Table 6.

Table 4. Comparison between Exact and Numerical Solutions, and Absolute Error at Time t = 1 for The Kink-Like Wave Case

$x(i)$	Exact	MOL-RK4	MOL-IRK5	Absolute Error MOL-RK4	Absolute Error MOL-IRK5
-80.0	1.9999991×10^{-1}	1.9999991×10^{-1}	1.9999991×10^{-1}	5.50×10^{-10}	5.50×10^{-10}
-79.5	1.9999990×10^{-1}	1.9999989×10^{-1}	1.9999989×10^{-1}	1.06×10^{-8}	1.06×10^{-8}
-79.0	1.9999989×10^{-1}	1.9999988×10^{-1}	1.9999988×10^{-1}	8.03×10^{-9}	7.98×10^{-9}
-78.5	1.9999988×10^{-1}	1.9999988×10^{-1}	1.9999988×10^{-1}	3.24×10^{-9}	3.29×10^{-9}
-78.0	1.9999987×10^{-1}	1.9999987×10^{-1}	1.9999987×10^{-1}	3.42×10^{-9}	3.43×10^{-9}
-77.5	1.9999986×10^{-1}	1.9999986×10^{-1}	1.9999986×10^{-1}	3.95×10^{-10}	2.90×10^{-10}
-77.0	1.9999984×10^{-1}	1.9999984×10^{-1}	1.9999984×10^{-1}	1.75×10^{-9}	1.88×10^{-9}
-76.5	1.9999983×10^{-1}	1.9999983×10^{-1}	1.9999983×10^{-1}	5.92×10^{-10}	6.48×10^{-10}
-76.0	1.9999981×10^{-1}	1.9999981×10^{-1}	1.9999981×10^{-1}	1.23×10^{-9}	1.15×10^{-9}
-75.5	1.9999979×10^{-1}	1.9999980×10^{-1}	1.9999980×10^{-1}	9.22×10^{-10}	7.40×10^{-10}
75.5	2.1×10^{-7}	2.1×10^{-7}	2.1×10^{-7}	2.81×10^{-9}	3.04×10^{-9}
76.0	1.9×10^{-7}	1.9×10^{-7}	1.9×10^{-7}	7.06×10^{-10}	5.64×10^{-10}
76.5	1.7×10^{-7}	1.7×10^{-7}	1.7×10^{-7}	4.80×10^{-9}	5.01×10^{-9}
77.0	1.6×10^{-7}	1.5×10^{-7}	1.5×10^{-7}	7.87×10^{-9}	7.89×10^{-9}
77.5	1.4×10^{-7}	1.4×10^{-7}	1.4×10^{-7}	8.65×10^{-9}	8.50×10^{-9}
78.0	1.3×10^{-7}	1.2×10^{-7}	1.2×10^{-7}	6.54×10^{-9}	6.61×10^{-9}
78.5	1.2×10^{-7}	1.2×10^{-7}	1.2×10^{-7}	1.65×10^{-9}	1.70×10^{-9}
79.0	1.1×10^{-7}	1.2×10^{-7}	1.2×10^{-7}	5.45×10^{-9}	5.50×10^{-9}
79.5	1.0×10^{-7}	1.1×10^{-7}	1.1×10^{-7}	1.39×10^{-8}	1.39×10^{-8}
80.0	9.0×10^{-8}	9.0×10^{-8}	9.0×10^{-8}	5.54×10^{-10}	5.54×10^{-10}

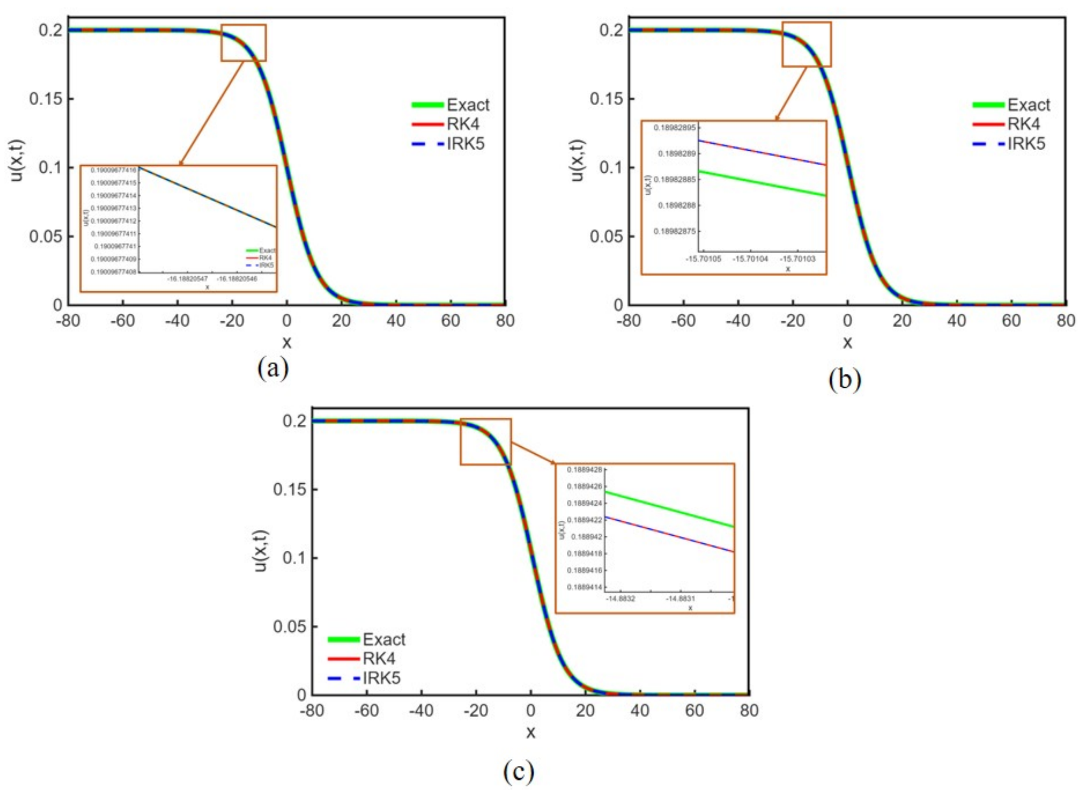

Figure 2. Exact and Numerical Solutions of The Gardner Equation Kink-Like Wave for δx = 0.5 at (a) t= 1, (b) t= 10, and (c) t= 20

Table 5. Comparison between Exact and Numerical Solutions, and Absolute Error at Time $t = 10$ for The Kink-Like Wave Case

$x(i)$	Exact	MOL-RK4	MOL-IRK5	Absolute Error MOL-RK4	Absolute Error MOL-IRK5
-80.0	1.9999991×10^{-1}	1.9999991×10^{-1}	1.9999991×10^{-1}	5.36×10^{-9}	5.36×10^{-9}
-79.5	1.9999991×10^{-1}	1.9999988×10^{-1}	1.9999988×10^{-1}	3.05×10^{-8}	3.05×10^{-8}
-79.0	1.9999990×10^{-1}	1.9999987×10^{-1}	1.9999987×10^{-1}	2.55×10^{-8}	2.55×10^{-8}
-78.5	1.9999989×10^{-1}	1.9999987×10^{-1}	1.9999987×10^{-1}	1.95×10^{-8}	1.95×10^{-8}
-78.0	1.9999988×10^{-1}	1.9999986×10^{-1}	1.9999986×10^{-1}	1.64×10^{-8}	1.64×10^{-8}
-77.5	1.9999987×10^{-1}	1.9999985×10^{-1}	1.9999985×10^{-1}	1.20×10^{-8}	1.20×10^{-8}
-77.0	1.9999985×10^{-1}	1.9999984×10^{-1}	1.9999984×10^{-1}	1.03×10^{-8}	1.03×10^{-8}
-76.5	1.9999984×10^{-1}	1.9999983×10^{-1}	1.9999983×10^{-1}	7.13×10^{-9}	7.13×10^{-9}
-76.0	1.9999982×10^{-1}	1.9999982×10^{-1}	1.9999982×10^{-1}	6.41×10^{-9}	6.41×10^{-9}
-75.5	1.9999981×10^{-1}	1.9999980×10^{-1}	1.9999980×10^{-1}	4.02×10^{-9}	4.02×10^{-9}
75.5	2.2×10^{-7}	2.0×10^{-7}	2.0×10^{-7}	1.44×10^{-8}	1.43×10^{-8}
76.0	2.0×10^{-7}	1.9×10^{-7}	1.9×10^{-7}	1.24×10^{-8}	1.24×10^{-8}
76.5	1.8×10^{-7}	1.8×10^{-7}	1.8×10^{-7}	3.58×10^{-9}	3.59×10^{-9}
77.0	1.7×10^{-7}	1.7×10^{-7}	1.7×10^{-7}	1.22×10^{-9}	1.22×10^{-9}
77.5	1.5×10^{-7}	1.6×10^{-7}	1.6×10^{-7}	1.16×10^{-8}	1.16×10^{-8}
78.0	1.4×10^{-7}	1.6×10^{-7}	1.6×10^{-7}	1.85×10^{-8}	1.85×10^{-8}
78.5	1.3×10^{-7}	1.6×10^{-7}	1.6×10^{-7}	3.02×10^{-8}	3.02×10^{-8}
79.0	1.2×10^{-7}	1.6×10^{-7}	1.6×10^{-7}	3.94×10^{-8}	3.94×10^{-8}
79.5	1.1×10^{-7}	1.6×10^{-7}	1.6×10^{-7}	5.22×10^{-8}	5.22×10^{-8}
80.0	1.0×10^{-7}	9.0×10^{-8}	9.0×10^{-8}	5.69×10^{-9}	5.69×10^{-9}

Table 6. Comparison between Exact and Numerical Solutions, and Absolute Error at Time $t = 20$ for The Kink-Like Wave Case

$x(i)$	Exact	MOL-RK4	MOL-IRK5	Absolute Error MOL-RK4	Absolute Error MOL-IRK5
-80.0	1.9999992×10^{-1}	1.9999991×10^{-1}	1.9999991×10^{-1}	1.04×10^{-8}	1.04×10^{-8}
-79.5	1.9999991×10^{-1}	1.9999987×10^{-1}	1.9999987×10^{-1}	3.94×10^{-8}	3.91×10^{-8}
-79.0	1.9999990×10^{-1}	1.9999987×10^{-1}	1.9999987×10^{-1}	3.37×10^{-8}	3.35×10^{-8}
-78.5	1.9999989×10^{-1}	1.9999987×10^{-1}	1.9999987×10^{-1}	2.70×10^{-8}	2.76×10^{-8}
-78.0	1.9999988×10^{-1}	1.9999986×10^{-1}	1.9999986×10^{-1}	2.33×10^{-8}	2.28×10^{-8}
-77.5	1.9999987×10^{-1}	1.9999985×10^{-1}	1.9999985×10^{-1}	1.88×10^{-8}	1.87×10^{-8}
-77.0	1.9999986×10^{-1}	1.9999984×10^{-1}	1.9999984×10^{-1}	1.71×10^{-8}	1.72×10^{-8}
-76.5	1.9999985×10^{-1}	1.9999983×10^{-1}	1.9999983×10^{-1}	1.33×10^{-8}	1.37×10^{-8}
-76.0	1.9999983×10^{-1}	1.9999982×10^{-1}	1.9999982×10^{-1}	1.17×10^{-8}	1.18×10^{-8}
-75.5	1.9999982×10^{-1}	1.9999981×10^{-1}	1.9999981×10^{-1}	8.02×10^{-9}	7.16×10^{-9}
75.5	2.3×10^{-7}	2.3×10^{-7}	2.3×10^{-7}	1.65×10^{-9}	1.94×10^{-9}
76.0	2.1×10^{-7}	2.2×10^{-7}	2.3×10^{-7}	1.23×10^{-8}	1.23×10^{-8}
76.5	1.9×10^{-7}	2.2×10^{-7}	2.2×10^{-7}	2.95×10^{-8}	2.96×10^{-8}
77.0	1.8×10^{-7}	2.2×10^{-7}	2.2×10^{-7}	4.55×10^{-8}	4.57×10^{-8}
77.5	1.6×10^{-7}	2.3×10^{-7}	2.3×10^{-7}	6.37×10^{-8}	6.34×10^{-8}
78.0	1.5×10^{-7}	2.3×10^{-7}	2.3×10^{-7}	7.97×10^{-8}	7.97×10^{-8}
78.5	1.3×10^{-7}	2.3×10^{-7}	2.3×10^{-7}	9.70×10^{-8}	9.74×10^{-8}
79.0	1.2×10^{-7}	2.3×10^{-7}	2.3×10^{-7}	1.11×10^{-7}	1.11×10^{-7}
79.5	1.1×10^{-7}	2.4×10^{-7}	2.4×10^{-7}	1.25×10^{-7}	1.25×10^{-7}
80.0	1.0×10^{-7}	9.0×10^{-8}	9.0×10^{-8}	1.17×10^{-8}	1.17×10^{-8}

3.3 Global Error Analysis

The accuracy of the numerical solutions for both solitary pulse and kink-like wave cases is evaluated using global error measures, including the maximum error, the mean absolute error, and the root mean square error. These error metrics are computed by comparing the numerical solutions with the corresponding exact solutions at selected time levels. The global error values for the solitary pulse and kink-like wave are reported in Table 7 and Table 8, respectively, while the error evolution is illustrated in Figure 3 and Figure 4.

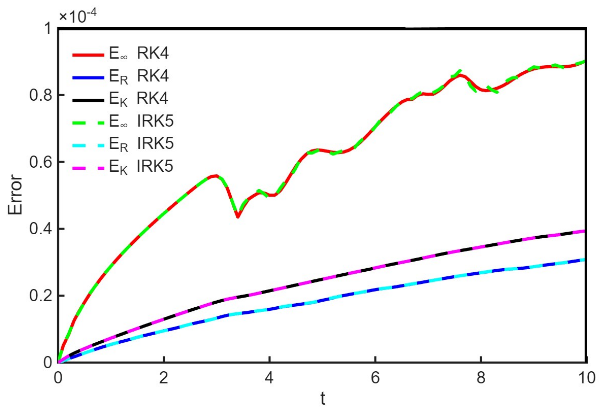

Figure 3. Global Error Evolution Over Time for The Gardner Equation Solitary Pulse

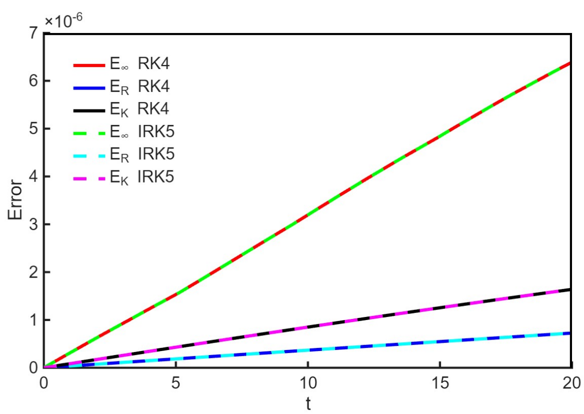

Figure 4. Global Error Evolution Over Time for The Gardner Equation Kink-Like Wave

For the solitary pulse case, the global error values exhibit a gradual increase as time progresses due to the accumulation of discretization errors. The magnitude of the errors remains small throughout the simulation interval, indicating that the numerical approximation retains a high level of accuracy. As shown in Figure 3, the error evolution for both MOL-RK4 and MOL-IRK5 follows a nearly identical trajectory, with E_∞ oscillating slightly but remaining below 1.0×10^{-4} up to $t = 10$. Table 8 highlights that at $t = 10$, the MOL-IRK5 scheme achieves an E_∞ of 9.0284×10^{-5}, which is slightly lower than the 9.0379×10^{-5} produced by MOL-RK4. This indicates that while both methods are highly accurate, the fifth-order refinement in IRK5 provides a marginal gain in suppressing long-term error accumulation.

For the kink-like wave case, the global error values are significantly smaller, reflecting enhanced numerical stability for this type of solution. Data from Table 8 shows that the maximum error (E_∞) for the kink-like wave is in the magnitude of 10^{-6} to 10^{-7}, which is two orders of magnitude smaller than the solitary pulse case. Figure 4 confirms a linear growth in error over time, yet the MOL-IRK5 scheme consistently maintains a level of precision that is virtually indistinguishable from or superior to the standard RK4, with E_∞ values reaching only 3.1959×10^{-6} at $t = 10$. The consistently low error levels in both cases demonstrate the reliability of the proposed numerical scheme.

The comparison of error behavior between the two cases highlights the effectiveness of the MOL-IRK5 approach across different solution characteristics. The observed error magnitudes confirm that the numerical scheme provides accurate approximations for both localized and transition type wave solutions of the Gardner equation. A detailed error summary at each observation time is given in Table 7 and Table 8.

3.4 Discussion on Accuracy and Efficiency of the MOL-IRK5 Scheme

The numerical results for the solitary pulse and kink-like wave cases indicate that the MOL-IRK5 scheme provides accurate approximations of the Gardner equation solutions. While both the MOL-RK4 and MOL-IRK5 schemes closely match the exact solutions, the MOL-IRK5 method demonstrates a more refined alignment with the exact wave profile, particularly at the peak of the solitary pulse and the steep transition of the kink-like wave. The numerical solutions closely match the exact solutions and preserve the wave profiles during propagation, demonstrating the reliability of the proposed MOL-IRK5 scheme. Figure 4 provides an additional visualization of the agreement between the numerical and exact solutions, reinforcing the accuracy of the MOL-IRK5 scheme.

Wave profiles preserve their shapes during propagation along the spatial domain. Global error values remain small over the entire time interval for both methods, however the MOL-IRK5 scheme generally yields lower absolute errors at specific spatial nodes than the standard RK4. No numerical oscillations appear throughout the simulations. Global error values remain small over the entire time interval. These observations demonstrate the reliability of the proposed numerical approach.

The accuracy of the numerical scheme is supported by the behavior of global error measures presented in the numerical results. The maximum error, meaning absolute error, and root mean square error increase gradually as time progresses. Such behavior is expected due to the accumulation of discretization errors in space and time, as reported in previous numerical studies of nonlinear dispersive equations (Hepson et al., 2020). The MOL-IRK5 scheme exhibits a slower rate of error growth compared to MOL-RK4. Table 8 reveals that for the solitary pulse at $t = 10$, the maximum error (E_∞) for IRK5 is 9.0284×10^{-5}, outperforming the RK4 value of 9.0379×10^{-5}. This

Table 7. Global Error Values at Specific Times for The Solitary Pulse Case

Time (t)	E_∞ RK4	E_∞ IRK5	E_R RK4	E_R IRK5	E_K RK4	E_K IRK5
1.0	2.8843×10^{-05}	2.8846×10^{-05}	5.4219×10^{-06}	5.4391×10^{-06}	7.3079×10^{-06}	7.3171×10^{-06}
2.0	4.4592×10^{-05}	4.4582×10^{-05}	9.4836×10^{-06}	9.4836×10^{-06}	1.2971×10^{-05}	1.2978×10^{-05}
3.0	5.5825×10^{-05}	5.5828×10^{-05}	1.3311×10^{-05}	1.3308×10^{-05}	1.8122×10^{-05}	1.8128×10^{-05}
4.0	5.0046×10^{-05}	4.9078×10^{-05}	1.5925×10^{-05}	1.5903×10^{-05}	2.1465×10^{-05}	2.1477×10^{-05}
5.0	6.3468×10^{-05}	6.4030×10^{-05}	1.8622×10^{-05}	1.8655×10^{-05}	2.4928×10^{-05}	2.4937×10^{-05}
6.0	7.0551×10^{-05}	7.0527×10^{-05}	2.1802×10^{-05}	2.1792×10^{-05}	2.8301×10^{-05}	2.8314×10^{-05}
7.0	8.0217×10^{-05}	8.0281×10^{-05}	2.4330×10^{-05}	2.4317×10^{-05}	3.1581×10^{-05}	3.1589×10^{-05}
8.0	8.1565×10^{-05}	8.2182×10^{-05}	2.6868×10^{-05}	2.6888×10^{-05}	3.4561×10^{-05}	3.4568×10^{-05}
9.0	8.7831×10^{-05}	8.8434×10^{-05}	2.8667×10^{-05}	2.8664×10^{-05}	3.7291×10^{-05}	3.7299×10^{-05}
10.0	9.0379×10^{-05}	9.0284×10^{-05}	3.0854×10^{-05}	3.0877×10^{-05}	3.9408×10^{-05}	3.9399×10^{-05}

Table 8. Global Error Values at Specific Times for The Kink-Like Wave Case

Time (t)	E_∞ RK4	E_∞ IRK5	E_R RK4	E_R IRK5	E_K RK4	E_K IRK5
1.0	3.1439×10^{-07}	3.1439×10^{-07}	3.7567×10^{-08}	3.7569×10^{-08}	8.6301×10^{-08}	8.6301×10^{-08}
2.0	6.2529×10^{-07}	6.2529×10^{-07}	7.4958×10^{-08}	7.4963×10^{-08}	1.7251×10^{-07}	1.7251×10^{-07}
3.0	9.2992×10^{-07}	9.2992×10^{-07}	1.1208×10^{-07}	1.1208×10^{-07}	2.5855×10^{-07}	2.5855×10^{-07}
4.0	1.2330×10^{-06}	1.2330×10^{-06}	1.4910×10^{-07}	1.4910×10^{-07}	3.4436×10^{-07}	3.4436×10^{-07}
5.0	1.5319×10^{-06}	1.5319×10^{-06}	1.8592×10^{-07}	1.8592×10^{-07}	4.2985×10^{-07}	4.2985×10^{-07}
6.0	1.8582×10^{-06}	1.8584×10^{-06}	2.2249×10^{-07}	2.2249×10^{-07}	5.1496×10^{-07}	5.1496×10^{-07}
7.0	2.1921×10^{-06}	2.1922×10^{-06}	2.5910×10^{-07}	2.5911×10^{-07}	5.9962×10^{-07}	5.9962×10^{-07}
8.0	2.5265×10^{-06}	2.5264×10^{-06}	2.9549×10^{-07}	2.9549×10^{-07}	6.8378×10^{-07}	6.8378×10^{-07}
9.0	2.8587×10^{-06}	2.8587×10^{-06}	3.3165×10^{-07}	3.3165×10^{-07}	7.6738×10^{-07}	7.6738×10^{-07}
10.0	3.1965×10^{-06}	3.1959×10^{-06}	3.6776×10^{-07}	3.6776×10^{-07}	8.5037×10^{-07}	8.5037×10^{-07}

behavior confirms the superior numerical stability of the MOL-IRK5 scheme for long-term integration.

The solitary pulse case shows that the numerical method effectively preserves localized traveling wave structures. Compared to the classical RK4, the IRK5 scheme more accurately follows the exact solitary pulse as it propagates (Mihalache, 2021), maintaining the wave's amplitude and width with higher fidelity. Although small deviations observed at later times are caused by accumulated numerical errors. These deviations do not significantly alter the overall wave profile (Qi et al., 2024).

Table 9. Convergence Results Obtained for Different Grid Resolutions

Δx	Kink-Like Waves Case		Solitary Pulse Case	
	Error	Order	Error	Order
1	6.180927×10^{-7}	–	2.690838×10^{-5}	–
0.5	1.574208×10^{-7}	1.9732	7.368389×10^{-6}	1.8686
0.25	3.953863×10^{-8}	1.9933	1.891260×10^{-6}	1.9620
0.125	9.895997×10^{-9}	1.9983	7.378937×10^{-7}	1.3579

The results confirm that the scheme performs well for localized wave solutions of the Gardner equation.

The kink-like wave case highlights the robustness of the numerical method for solutions with sharp transition regions. The MOL-IRK5 scheme captures the monotonic structure of the kink-like wave with exceptional precision, producing global error values (Table 8) that are significantly smaller than those obtained for the solitary pulse case. When compared to RK4, the IRK5 scheme consistently maintains lower L_∞ and L_2 norms, indicating enhanced numerical stability when handling steep gradients (Mandikas and Voulgarakis, 2025).

The efficiency of the MOL- IRK5 scheme is achieved through the combination of spatial discretization and high-order time integration. While both MOL-RK4 and MOL-IRK5 are constrained by the second-order spatial discretization, the IRK5 time-stepping provides a more accurate temporal evolution, leading to smaller global errors, especially in the kink-like wave case where monotonic structures reduce numerical dispersion. This combination makes the scheme more suitable for practical numerical studies requiring a balance between computational cost and high-order precision (Liu et al., 2022). The smaller global errors observed in the kink-like wave case can be attributed to the monotonic structure of the solution, which reduces numerical dispersion effects compared to localized solitary pulse solutions. Although the Improved Runge-Kutta method provides fifth-order accuracy in time, the overall accuracy of the numerical scheme is mainly governed by the second-order spatial discretization. Consequently, the combined MOL-IRK5 scheme demonstrates approximately second-order convergence with respect to spatial grid refinement.

3.5 Convergence Analysis

To verify the accuracy of the proposed numerical scheme, a convergence test is conducted using progressively refined spatial grids. The numerical error is evaluated using the maximum norm defined in Equation (19). The experimental order of convergence is calculated using Equation (22):

$$p = \frac{\log\left(\frac{E_1}{E_2}\right)}{\log\left(\frac{h_1}{h_2}\right)} \tag{22}$$

where E_1 and E_2 represent numerical errors corresponding to grid sizes h_1 and h_2.

Table 9 confirms that the numerical scheme exhibits approximately second-order convergence, which is consistent with the spatial discretization used in the Method of Lines.

4. CONCLUSIONS

This study has successfully developed and implemented a numerical scheme based on the Method of Lines combined with an Improved Runge-Kutta method of order five (MOL-IRK5) to solve the Gardner equation. The application of second-order central finite difference spatial discretization and fifth-order time integration to solitary pulse and kink-like wave cases demonstrated high accuracy and robust numerical performance. A key finding is that the MOL-IRK5 scheme consistently outperforms the classical MOL-RK4 method, yielding lower global error norms (E_∞, E_R, E_K) and showing superior stability in preserving wave profiles and sharp gradients over long-term simulations. These results confirm that the MOL-IRK5 approach provides a more precise and efficient framework for modeling nonlinear dispersive wave solutions compared to standard fourth-order schemes. While the overall accuracy is primarily governed by spatial discretization, the IRK5 temporal integrator ensures a more stable evolution, making it a reliable tool for investigating complex nonlinear evolution equations in fluid dynamics and related physical systems. Future work may focus on stability analysis, adaptive time stepping, and extension to higher-dimensional nonlinear evolution equations.

5. ACKNOWLEDGMENT

The authors acknowledge the Department of Mathematics, Faculty of Mathematics and Natural Sciences, Universitas Brawijaya, for academic support and research facilities. This research was funded by the Internal Grant of FMIPA Universitas Brawijaya under Contract Number: 06455.6/UN10.F0901/B/PT/2025 (Internal Funding Scheme B 2025).

REFERENCES

Bacca, J., E. Martinez, and H. Arguello (2023). Computational Spectral Imaging: A Contemporary Overview. *Journal of the Optical Society of America A*, **40**(4); C115–C125

Boyce, W. E. and R. C. DiPrima (2012). *Elementary Differential Equations and Boundary Value Problems*. John Wiley & Sons, Inc., New Jersey, 10 edition

Cox, S. M. and P. C. Matthews (2002). Exponential Time Differencing for Stiff Systems. *Journal of Computational Physics*, **176**(2); 430–455

Dahiya, S., A. Singh, and S. P. Singh (2023). Study of the Gardner Equation with Homogeneous Boundary Conditions via Fourth Order Modified Cubic B-Spline Collocation Method. *Computational Mathematics and Mathematical Physics*, **63**(12); 2474–2491

Degon, L. and A. Chowdhury (2022). Approximate Solutions to the Gardner Equation by Spectral Modified Exponential Time Differencing Method. *Partial Differential Equations in Applied Mathematics*, **5**; 100310

Gardner, C. L. (2024). Numerical Methods for Mixed Type PDEs. In *Applied Numerical Methods for Partial Differential Equations*. Springer Nature Switzerland, Cham, pages 185–200

Habibah, U., F. F. Medrano, A. C. Permana, D. Ardiana, and Trisilowati (2025). An Improved Fifth-Order Runge-Kutta Method with Higher Accuracy and Efficiency for Solving Initial Value Problems. *Science and Technology Indonesia*, **10**(3); 802–816

Hepson, O. E., A. Korkmaz, and I. Dag (2018). Numerical Solutions of the Gardner Equation by Extended Form of the Cubic B-Splines. *Pramana*, **91**(4); 1–13

Hepson, O. E., A. Korkmaz, and I. Dag (2020). Exponential B-Spline Collocation Solutions to the Gardner Equation. *International Journal of Computer Mathematics*, **97**(4); 837–850

Ji, Y. and Y. Xing (2023). Highly Accurate and Efficient Time Integration Methods with Unconditional Stability and Flexible Numerical Dissipation. *Mathematics*, **11**(3); 593

Kai, Y., S. Chen, K. Zhang, and Z. Yin (2024). A Study of the Shallow Water Waves with Some Boussinesq-Type Equations. *Waves in Random and Complex Media*, **34**(3); 1251–1268

Kassam, A. K. and L. N. Trefethen (2005). Fourth-Order Time-Stepping for Stiff PDEs. *SIAM Journal on Scientific Computing*, **26**(4); 1214–1233

Keppens, R., B. P. Braileanu, Y. Zhou, W. Ruan, C. Xia, Y. Guo, and F. Bacchini (2023). MPI-AMRVAC 3.0: Updates to an Open-Source Simulation Framework. *Astronomy & Astrophysics*, **673**; A66

Khater, M. M. (2024). Dynamics of Nonlinear Time Fractional Equations in Shallow Water Waves. *International Journal of Theoretical Physics*, **63**(4); 92

Liu, Y., J. N. Kutz, and S. L. Brunton (2022). Hierarchical Deep Learning of Multiscale Differential Equation Time-Steppers. *Philosophical Transactions of the Royal Society A*, **380**(2229); 20210200

Mandikas, V. G. and A. Voulgarakis (2025). High-Resolution Numerical Scheme for Simulating Wildland Fire Spread. *Mathematics*, **13**(22); 3721

Mihalache, D. (2021). Localized Structures in Optical and Matter-Wave Media: A Selection of Recent Studies. *Romanian Reports in Physics*, **73**(2); 403

Neto, A. B., W. J. Mansur, and W. G. Ferreira (2022). Spurious Oscillations Reduction in Transient Diffusion and Wave Propagation Problems Discretized with the Finite Element Method. *Scientific Reports*, **12**(1); 18887

Qi, Y., Y. Tian, and Y. Jiang (2024). Existence of Traveling Wave Solutions for the Perturbed Modified Gardner Equation. *Qualitative Theory of Dynamical Systems*, **23**(3); 106

Rugg, N., J. F. Mahlmann, and A. Spitkovsky (2024). Safety First: Stability and Dissipation of Line-Tied Force-Free Flux Tubes in Magnetized Coronae. *The Astrophysical Journal*, **966**(2); 173

Shu, C.-W. (2009). High-Order Methods for Hyperbolic PDEs. *SIAM Review*, **51**(1); 82–126

Tiong, W. K., K. G. Tay, C. T. Ong, and S. N. Sze (2017). Numerical Solution of the Gardner Equation. In *Proceedings of the International Conference on Computational Mathematics and Statistics (iCMS 2015)*. Springer, Singapore, pages 243–251

Trisilowati, I., U. Darti, U. Habibah, and O. D. Wijaya (2021). *Metode Numerik dengan MATLAB*. UB Press, Malang, 1 edition

Wazwaz, A. M. (2009). *Partial Differential Equations and Solitary Waves Theory*. Springer, Heidelberg

Wu, X. L. and Y. Zhao (2024). A Novel Heat Pulse Method in Determining "Effective" Thermal Properties in Frozen Soil. *Water Resources Research*, **60**(12); e2024WR037537

Yang, H. (2024). Improving Prediction Accuracy of Laser-Induced Shock Wave Velocity Prediction Using Neural Networks. *Scientific Reports*, **14**(1); 13576

Zhang, Y., L. Gui, and B. Feng (2025). Solutions of Cauchy Problems for the Gardner Equation in Three Spatial Dimensions. *Symmetry*, **17**(1); 102